Precise Guidance and Attitude Control Systems for the Information Satellites: Results and New Challenges*

Yevgeny I. Somov *

* *Samara Scientific Center, Russian Academy of Sciences (RAS)*
3a Studenchesky Lane, Samara 443001 Russia
(e-mail: e_somov@mail.ru)

Abstract: Mathematical methods for research and designing the attitude control systems by information spacecraft, are considered. Some results and new challenges for perspective spacecraft are presented.

Keywords: information spacecraft, precise attitude control

1. INTRODUCTION

During the recent 3 decades Department "Dynamics and Motion Control" of Samara Scientific Center RAS have accumulated substantial practical experience in research and designing the aerospace guidance, navigation and flight control systems. This paper briefly presents the research results achieved by the Department only on the attitude control systems for Russian information satellites (Fig. 1 and Fig. 2), and also new challenges for perspective spacecraft by this class.

2. ROBUST NONLINEAR CONTROL

Applied general approach to synthesis of *nonlinear* control system (NCS) with a partial measurement of its state is presented, moreover the method of *vector Lyapunov functions* (VLF), which has a strong mathematical basis for analysis of stability of various nonlinear interconnected systems with the *discontinuous right-hand side*, is used in cooperation with the *exact feedback linearization* (EFL) technique. Let there be given a nonlinear controlled object

$$D^+\mathrm{x}(t)=\mathcal{F}(\mathrm{x}(t),\mathrm{u});\quad \mathrm{x}(t_0)=\mathrm{x}_0;\ t\in \mathrm{T}_{t_0},$$

where $\mathrm{x}(t)\in\mathcal{H}\subset\mathbb{R}^n$ is a state vector with an initial condition $\mathrm{x}_0\in\mathcal{H}_0\subseteq\mathcal{H}$; $\mathrm{u}=\{u_j\}\in\mathrm{U}\subset\mathbb{R}^r$ is a control vector. Let some *vector norms* $\rho(\mathrm{x})\in\overline{\mathbb{R}}^l_+$ and $\rho^0(\mathrm{x}_0)\in\overline{\mathbb{R}}^{l_0}_+$ also be *given*. For any control law (CL) $\mathrm{u}=\mathcal{U}(\mathrm{x})$ the closed-loop system has the form

$$D^+\mathrm{x}(t)=\mathcal{X}(t,\mathrm{x});\quad \mathrm{x}(t_0)=\mathrm{x}_0, \tag{1}$$

where $\mathcal{X}(t,\mathrm{x})=\mathcal{F}(\mathrm{x},\mathcal{U}(\mathrm{x})),\mathcal{X}:\mathrm{T}_{t_0}\times\mathcal{H}\to\mathcal{H}$ is a *discontinuous* operator. Assuming the existence and the non-local continuability of the *right-sided* solution $x(t)\equiv\mathrm{x}(t_0,\mathrm{x}_0;t)$ of the system (1) for its *extended definition* in the aspect of physics, the most important dynamic property is obtained, that is $\rho\rho^0$-*exponential invariance* of the solution $x(t)=0$ under the *desired* $\gamma\in\overline{\mathbb{R}}^l_+$:

* The work was supported by the RFBR (Grant 08-08-00512) and Division on EMMCP of the RAS (Program 15).

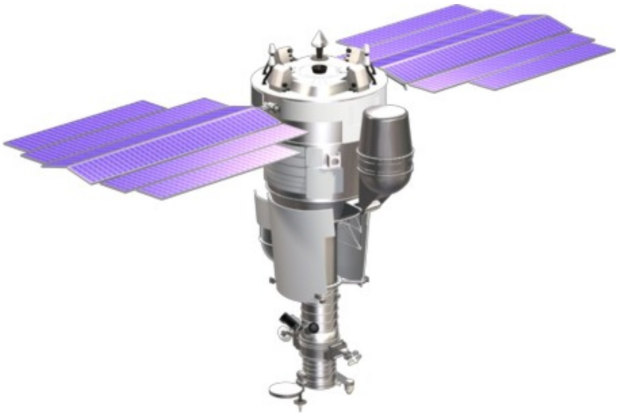

Fig. 1. The observation spacecraft *Resourse-DK1*

Fig. 2. The communication spacecraft *Sesat*

$$(\exists\alpha\in\mathbb{R}_+)\,(\exists\mathcal{B}\in\overline{\mathrm{B}}^{l\times l_0}_+)\,(\exists\delta\in\mathbb{R}^{l_0}_+)\,(\forall\rho^0(\mathrm{x}_0)<\delta)$$
$$\rho(x(t))\le\gamma+\mathcal{B}\ \rho^0(\mathrm{x}_0)\ \exp(-\alpha(t-t_0))\quad\forall t\in\mathrm{T}_{t_0}.$$

For the VLF $\upsilon:\mathcal{H}\to\overline{\mathbb{R}}^k_+$ with components $\upsilon^s(\mathrm{x})\ge 0$, $\upsilon^s(0)=0$, $s=1:k$ and the norm $\|\upsilon(\mathrm{x})\|=\max\{\upsilon^s(\mathrm{x})\}$, defined are scalar function $\overline{\upsilon}(\mathrm{x})=\max\{\upsilon^s(\mathrm{x}),s=1:l_k,1\le$

$l_k \le k\}$ and a υ *upper right derivative* with respect to (1):

$$\overline{\upsilon}'(\mathrm{x}) \equiv \overline{\lim_{\delta t \to 0+}} \ (\upsilon(\mathrm{x} + \delta t\, \mathcal{X}(t,\mathrm{x})) - \upsilon(\mathrm{x}))/\delta t.$$

Theorem . *Let there exist the VLF* υ*, so that*:

1) $(\exists \mathrm{a} \in \mathbb{R}^l_+)\ (\forall \mathrm{x} \in \mathcal{H}) \qquad \rho(\mathrm{x}) \le \mathrm{a} \cdot \overline{\upsilon}(\mathrm{x})$;
2) $(\exists \mathrm{b} \in \mathbb{R}^{l_0}_+)\ (\forall \mathrm{x}_0 \in \mathcal{H}_0)\ \|\upsilon(\mathrm{x}_0)\| \le \langle \mathrm{b}, \rho^0(\mathrm{x}_0)\rangle$;
3) $\exists \gamma_c \in \overline{\mathbb{R}}^k_+$, *a function* $\varphi_\gamma(\cdot)$ *exists for* $\gamma_c \le \varphi_\gamma(\mathrm{a}, \gamma)$;
4) $\forall\ (t, \mathrm{x}) \in (\mathrm{T}_{t_0} \times \mathcal{H})$ *the conditions are satisfied*:
   a) $\overline{\upsilon}'_\gamma(\mathrm{x}) \le \mathrm{f}_c(t, \upsilon_\gamma(\mathrm{x})) \equiv \mathrm{P}\upsilon_\gamma(\mathrm{x}) + \tilde{\mathrm{f}}_c(t, \upsilon_\gamma(\mathrm{x}))$;
   b) Hurwitz condition for positive matrix P;
   c) Ważewski condition on quasi-monotonicity for the function $\tilde{\mathrm{f}}_c(t, \mathrm{y})$;
   d) Carateodory condition for the function $\tilde{\mathrm{f}}_c(t, \mathrm{y})$*, bounded in each domain* $\Omega^r_c = (\mathrm{T}_{t_0} \times \mathcal{S}^r_c)$*, where* $r > 0$ *and* $\mathcal{S}^r_c = \{\mathrm{y} \in \mathbb{R}^k : \|\mathrm{y}\|_{\mathrm{E}} < r\}$;
   e) $(\tilde{\mathrm{f}}_c(t, \mathrm{y})/\|\mathrm{y}\|) \overset{t \in \mathrm{T}_{t_0}}{\Longrightarrow} 0$ *for* $\mathrm{y} \to 0$ *uniformly with respect to time* $t \in \mathrm{T}_{t_0}$,

where $\upsilon_\gamma = \upsilon - \gamma_c$*. Then solution* $x(t) = 0$ *of the system* (1) *is* $\rho\rho^0$*-exponential invariant and the matrix* $\mathcal{B}$ *has the form* $\mathcal{B} = c \cdot \mathrm{ab}^{\mathrm{t}}$ *with* $c \in \mathbb{R}_+$.

There is such an important problem: by what approach is it possible to create *constructive* techniques for constructing the VLF $\upsilon(\mathrm{x})$ and *simultaneous* synthesis of a nonlinear control law $\mathrm{u} = \mathcal{U}(\mathrm{x})$ for the close-loop system (1) with given vector norms $\rho(\mathrm{x})$ and $\rho^0(\mathrm{x}_0)$? Recently, a pithy technique on constructing VLF at such synthesis has been elaborated. This method is based on a *nonlinear transformation* of the NCS model and solving the problem in two stages.

In stage 1, the right side $\mathcal{F}(\cdot)$ in (1) is transformed as $\mathcal{F}(\cdot) = \mathrm{f}(\mathrm{x}) + \mathrm{G}(\mathrm{x})\,\mathrm{u} + \tilde{\mathcal{F}}(t, \mathrm{x}(t), \mathrm{u})$, some *principal variables* in a state vector $\mathrm{x} \in \tilde{\mathcal{H}} \subset \mathbb{R}^{\tilde{n}} \subseteq \mathbb{R}^n$ with $\tilde{n} \le n$, $\mathrm{x}_0 \in \tilde{\mathcal{H}}_0 \subseteq \tilde{\mathcal{H}}$ are selected and a *simplified nonlinear model* of the object (1) is presented in the form of an affine *quite smooth* nonlinear control system

$$\dot{\mathrm{x}} = \mathrm{F}(\mathrm{x}, \mathrm{u}) \equiv \mathrm{f}(\mathrm{x}) + \mathrm{G}(\mathrm{x})\mathrm{u} \equiv \mathrm{f}(\mathrm{x}) + \sum \mathrm{g}_j(\mathrm{x}) u_j,$$

which is structurally synthesized by the EFL technique. In this aspect, based on the structural analysis of *given* vector norms $\rho(\mathrm{x})$ and $\rho^0(\mathrm{x})$, and also vector-functions $\mathrm{f}(\mathrm{x})$ and $\mathrm{g}_j(\mathrm{x})$, the *output vector-function* $\mathrm{h}(\mathrm{x}) = \{\mathrm{h}_i(\mathrm{x})\}$ is carefully selected. Furthermore, the nonlinear invertible (one-to-one) coordinate transformation $\mathrm{z} = \Phi(\mathrm{x})\ \forall \mathrm{x} \in \mathcal{S}_{\mathrm{h}} \subseteq \tilde{\mathcal{H}}$ with $\Phi(0) = 0$ is analytically obtained with *simultaneous* constructing the VLF. Finally, bilateral component-wise inequalities for the vectors $\mathrm{x}, z, \upsilon(\mathrm{x}), \rho(\mathrm{x}), \rho^0(\mathrm{x}_0)$ are derived, it is most desirable to obtain the *explicit* form for the nonlinear transformation $\mathrm{x} = \Psi(\mathrm{z})$, inverse with respect to $\mathrm{z} = \Phi(\mathrm{x})$, and the VLF aggregation procedure is carried out with analysis of proximity for a singular directions in the *Jacobian* $[\partial \mathrm{F}(\mathrm{x}, \mathcal{U}(\mathrm{x}))/\partial \mathrm{x}]$.

In stage 2, the problem of nonlinear CL synthesis for the *complete model* of the NCS (1), taking rejected coordinates, nonlinearities and restrictions on control, into account is solved by the VLF-method. If a forming control is digital, a measurement the model's state is discrete and incomplete, then a simplified nonlinear discrete object's model is obtained by *Teylor-Lie* series, a *nonlinear* digital CL is formed and its parametric synthesis is carried out with a simultaneously construct a *discrete sub-vector* VLF.

3. THE COMMUNICATION SATELLITE

The *S*iberian-*E*urope *Sat*ellite (*Sesat*) is a first communication spacecraft produced jointly by Russia and Europe. The *Sesat* was orbited on April 18, 2000. The *Sesat* attitude & orbit control system (AOCS) is based on the following configuration: the ES and the fine digital SS, the precise GU, a three-axial RG block, the GW, the SAP driver (AD) based on the GSDs, the RTs, Fig. 3. Electric plasma RTs are used for spacecraft station keeping, and hydrazine RTs — for attitude control and GW unloading.

3.1 Initial Orientation Modes

When the *Sesat* has been separated from *Proton* launcher, the Initial modes of Attitude Determination and Control System (ADCS) begin:

- Damping mode (DM) $\mapsto$ [RGs & RTs & AD]:
  - braking the angular rate vector $\boldsymbol{\omega}(t)$ at the inertial reference frame (IRF) $\mathbf{I}_\oplus$;
  - the SAPs turn to a fixed position when their normal $\mathbf{n}^p$ is oriented contrary the unit $\mathbf{b}_y$ of the body reference frame (BRF) $\mathbf{B} = \{\mathbf{b}_i\}$ $(\mathrm{O}xyz)$, see Fig. 3;
- Sun Acquisition mode (SAM) $\mapsto$ $[\,\cdot\,]$ & [SS]:
  - Sun unit $\mathbf{S}$ acquisition within one body revolution around the $-\mathbf{b}_y$ unit;
  - Sun pointing by a fixed unit $\mathbf{b}'_y$, Fig. 3;
- Earth Acquisition mode (EAM) $\mapsto$ $[\,\cdot\,]$&[ES]:
  - the satellite is rotated around the unit $\mathbf{b}'_y$ keeping the same Sun pointing;
  - Earth unit $\mathbf{E}$ acquisition by the ES;
- Preliminary Earth Orientation mode (EOPM) $\mapsto$ $[\,\cdot\,]$ & [AD & GW]:
  - GW rotor acceleration;
  - SAPs rotation in the Tracking mode.

The Earth Orientation mode (EOM) is used for the body three-axes orientation and stabilization in the ORF $\mathbf{I}_{\mathrm{o}}$ $(\mathrm{O}x^{\mathrm{o}}y^{\mathrm{o}}z^{\mathrm{o}})$ by the device base [ES & GW] with GW unloading by the RTs and for SAPs Sun pointing by the AD. A digital control law does not employ physical measurement of the yaw angle or its rate but certainly provides the body attitude control in the ORF using coupling roll and yaw channels.

Three Axes Stabilization mode (TASM) is the main nominal mode of ADCS operation. It has the device base [GU & GW & AD] with an infrequent calibration of the GU by the SS and ES digitally filtered signals. TASM provides precise body attitude stabilization in the ORF and the SAPs Sun pointing in three sub-modes:

- nominal sub-mode;
- GW momentum unloading (GWMU);
- station keeping manoeuvre (SKM).

The Twirl mode (TWM) is intended to provide positive power balance in an emergency case. Here the ADCS ensures a single-axis attitude stabilization of the SC body in the IRF by its rotation around the BRF Oz axis.

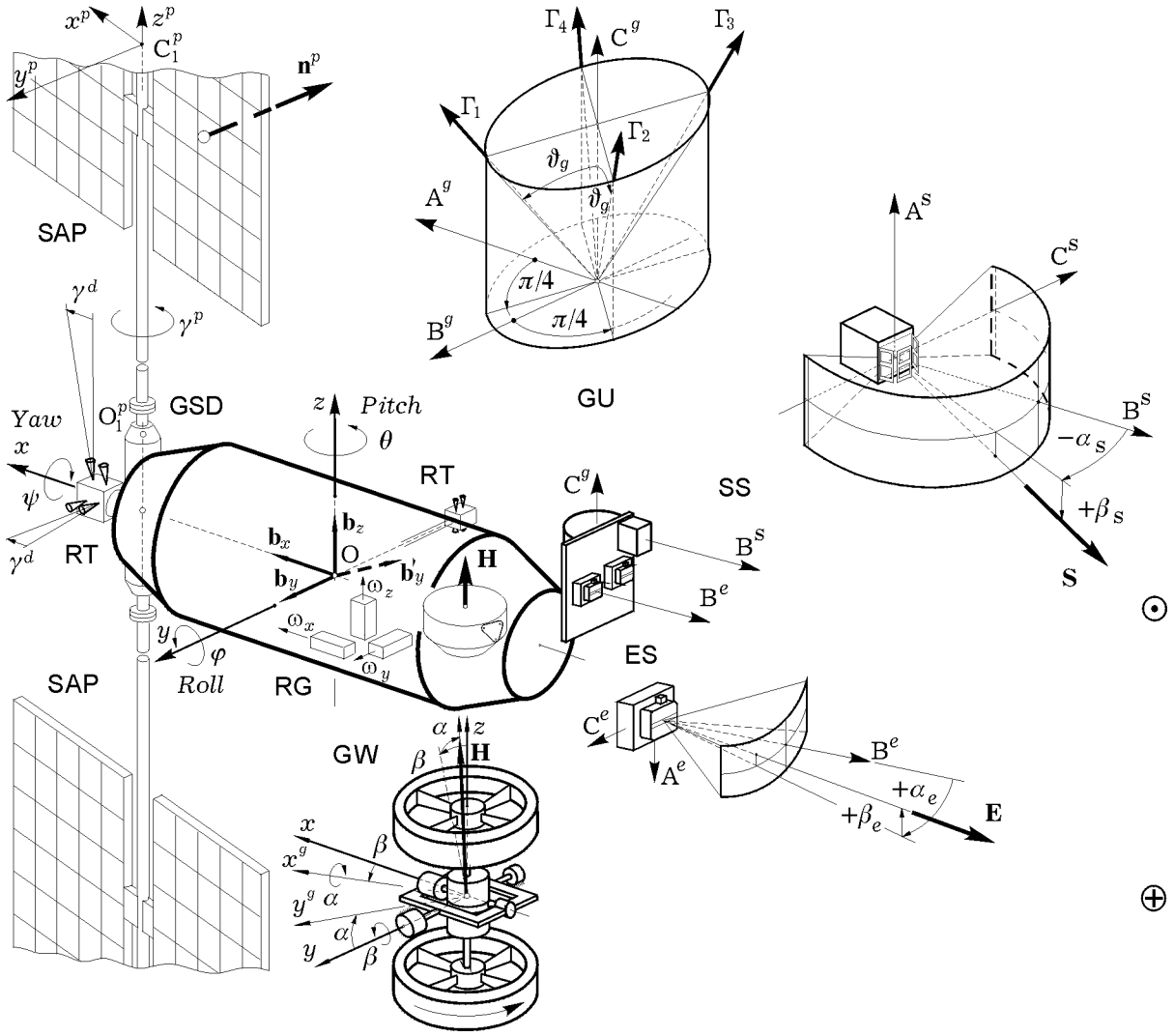

Fig. 3. The spacecraft *Sesat* onboard equipment layout scheme: ES — the Earth sensor; SS — the Sun sensor; GU — gyro unit; RG — rate gyrosensor; GW — gyrowheel (a momentum wheel mounted on 2-DOF gimbal); RT — reaction thruster; SAP — solar array panel; GSD — gear stepping drive.

3.2 Nonlinear Model of Body Attitude Motion

Position of the spacecraft mass center C on given circular orbit is defined by radius-vector $\mathbf{r}_o(t)$ with unit $\mathbf{r}^o$ and the true anomaly $\nu_o(t)$, which is combined with the orbit latitude $u_o(t) = \omega_\pi + \nu_o(t)$, where ω_π is a conventional latitude of orbit perigee. The BRF $\mathbf{B}$ attitude with respect to the ORF is defined by quaternion $\mathbf{\Lambda}^o = (\lambda_0^o, \boldsymbol{\lambda}^o)$ with $\boldsymbol{\lambda}^o = (\lambda_1^o, \lambda_2^o, \lambda_3^o)$, by angles of yaw ψ, roll φ and pitch θ (see Fig. 3) for the rotational sequence {1-3-2} and by matrix $\mathbf{T}_o^b = [\varphi]_2\,[\theta]_3\,[\psi]_1$, where $[\alpha]_i$ is well-known matrix of elementary rotation. The ORF angular rate vector $\boldsymbol{\omega}_o(t) = \dot{\boldsymbol{\nu}}_o(t)$ with respect to IRF $\mathbf{I}_\oplus$ have the form $\boldsymbol{\omega}_o^o = \{0, 0, \omega_o\}$ in the ORF and the representation $\boldsymbol{\omega}_o^b = \mathbf{T}_o^b\,\boldsymbol{\omega}_o^o$ in the BRF. At a body rate vector $\boldsymbol{\omega}(t) = \{\omega_i(t)\}$ the kinematic relations $\dot{\mathbf{\Lambda}}^o = (\mathbf{\Lambda}^o \circ \boldsymbol{\omega} - \boldsymbol{\omega}_o^o \circ \mathbf{\Lambda}^o)/2$ for quaternion $\mathbf{\Lambda}^o(t)$ and the Euler-Krylov angles of yaw ψ, roll φ and pitch θ

$$\begin{bmatrix} \dot\psi \\ \dot\varphi \\ \dot\theta \end{bmatrix} = \begin{bmatrix} (\omega_{xz} - \omega_o^o S_\psi S_\theta)/C_\theta \\ \omega_y + (\omega_{xz} S_\theta - \omega_o^o S_\psi)/C_\theta \\ -\omega_x S_\varphi + \omega_z C_\varphi - \omega_o^o C_\psi \end{bmatrix} \qquad (2)$$

with $\omega_{xz} \equiv \omega_x C_\varphi + \omega_z S_\varphi$ for the attitude angle vector $\boldsymbol{\alpha} = \{\alpha_i\} \equiv \{\psi, \varphi, \theta\}$, uniquely determine the *Sesat* BRF orientation in the ORF. Moreover, the attitude matrix $\mathbf{T}_o^b = \mathbf{I}_3 - 2[\boldsymbol{\lambda}^o\times]\mathbf{Q}_\lambda^{\mathrm{t}}$, where $\mathbf{Q}_\lambda = \mathbf{I}_3\lambda_0^o + [\boldsymbol{\lambda}^o\times]$ with $\det(\mathbf{Q}_\lambda) = \lambda_0^o$. At some simplified assumptions the nonlinear model of the *Sesat* body attitude dynamics is appeared as follows

$$\begin{bmatrix} \mathbf{J} & \mathbf{D}_q \\ \mathbf{D}_q^{\mathrm{t}} & \mathbf{A}^q \end{bmatrix} \cdot \begin{bmatrix} \dot{\boldsymbol{\omega}} \\ \ddot{\mathbf{q}} \end{bmatrix} = \begin{bmatrix} \mathbf{F}^\omega \\ \mathbf{F}^{\mathrm{q}} \end{bmatrix}, \qquad (3)$$

where $\mathbf{F}^\omega = -\boldsymbol{\omega} \times \mathbf{G} + \mathbf{M}_o^p + \mathbf{M}_o^{\mathrm{g}} + \mathbf{M}_o^{\mathrm{d}} + \mathbf{M}_o + \mathbf{Q}_o^{\mathrm{v}}$;

$\mathbf{F}^{\mathrm{q}} = -\mathbf{A}^q(\mathbf{S}_q\dot{\mathbf{q}} + \mathbf{W}_q\mathbf{q}) - \mathbf{P}_q^{\mathrm{t}}\ddot{\gamma}^p + \mathbf{Q}_q^{\mathrm{v}}$; $\mathbf{S}_q = \mathbf{V}_q + \mathbf{\Phi}_q$;

$\mathbf{G} = \mathbf{J}\,\boldsymbol{\omega} + \mathbf{D}_q\dot{\mathbf{q}} + \mathbf{H}$; $\mathbf{H} = \mathrm{H}\cdot\mathbf{h}_{\mathrm{g}}(\alpha,\beta)$; $\mathbf{M}_o^{\mathrm{g}} = -\dot{\mathbf{H}}$;

$\mathbf{h}_{\mathrm{g}} = \{C_\alpha S_\beta, -S_\alpha, C_\alpha C_\beta\}$; $\dot{\mathbf{H}} = \mathrm{H}\,\mathbf{A}_{\mathrm{h}}\{\dot\alpha, \dot\beta\} + \dot{\mathrm{H}}\,\mathbf{h}_{\mathrm{g}}$;

$\mathbf{V}_q = \mathbf{N}_q\mathbf{\Omega}_q$; $\mathbf{W}_q = \mathbf{\Omega}_q^2$; $\mathbf{N}_q = \lceil\nu_s^p\rfloor$; $\mathbf{\Omega}_q = \lceil\Omega_{\mathrm{s}}^{\mathrm{p}}\rfloor$;

$\nu_s^q = \delta_s^q/\pi$; $\mathbf{\Phi}_q = -(\mathbf{\Phi}_q)^{\mathrm{t}} = [\{\phi_{sl}\}]$, $\phi_{sl} = -2\mathbf{g}_{ls}^{\mathrm{t}}\cdot\boldsymbol{\omega}$;

$\mathbf{Q}_o^{\mathrm{v}} = -\mathbf{L}\times\mathbf{w}_o$; $\mathbf{Q}_q^{\mathrm{v}} = -\mathbf{M}_q^{\mathrm{t}}\mathbf{w}_o$; $\mathbf{w}_o = \overset{*}{\mathbf{v}}_o + \boldsymbol{\omega}\times\mathbf{v}_o$;

$$\mathbf{M}_o^p = \begin{bmatrix} (J_{xy}^{pd}(S_{2\gamma^p}\,\omega_x - C_{2\gamma^p}\,\omega_y) - 2J_z^p\omega_y)\cdot\dot\gamma^p \\ -(J_{xy}^{pd}(C_{2\gamma^p}\,\omega_x - S_{2\gamma^p}\,\omega_y) + 2J_z^p\omega_y)\cdot\dot\gamma^p \\ -2J_z^p\cdot\ddot\gamma^p \end{bmatrix};$$

$$J^{pd}_{xy} = J^{p}_{x} - J^{p}_{y};\quad \mathbf{M}^{\mathrm{d}}_{o} = \mathbf{M}^{do}_{o} + \mathbf{M}^{dk}_{o};\quad \mathbf{M}_{o} = \mathbf{M}^{gr}_{o} + \mathbf{M}^{s}_{o};\qquad \mathbf{A}_{\mathrm{h}} = \begin{bmatrix} C_\alpha C_\beta & -S_\alpha S_\beta \\ 0 & -C_\alpha \\ -C_\alpha S_\beta & -S_\alpha C_\beta \end{bmatrix},$$

the symbols $\circ$,$\tilde{}$ for quaternion, $\times$, $\{\cdot\} \equiv \mathrm{col}(\cdot)$, $[\cdot] \equiv \mathrm{line}(\cdot)$ for vectors and $[\cdot\times]$, $(\cdot)^{\mathrm{t}}$, $\lceil\cdot\rfloor \equiv \mathrm{diag}(\cdot)$ for matrix are conventional denotations.

3.3 Attitude Measurement and Estimation

Models of the *Sesat* body attitude state (the ES and the SS, the GU, the RG block), the GW and the SAPs state sensors take into account:

- their own dynamic properties;
- nonlinear static characteristics, for example because of constraint on the SS and the ES field of view ;
- noise, systematic and instrumental errors;
- time delays, time sampling, quantization and boundedness of their outputs;
- GU calibration by a digital observer based on the SS and the ES discrete filtered signals;
- possible faults and embedded diagnosis.

Digital observers are used for filtering the physical measurements of the body attitude angles and discrete dynamic estimation of the SC angular rate vector.

Attitude Reaction Thrusters The pulse-width modulation (PWM) model of a *normed* controlling torque $m^d_n(t)$ by any RT under an input command v^d_k taking into account a time delay T^d_{zu} is defined by the differential equation

$$\mathrm{T}^d \dot{m}^d_n(t) + m^d_n(t) = \mathrm{s}_k \cdot \mathrm{u}^n(t - T^d_{zu}, \tau_k, t_k), \tag{4}$$

where $t_k = k \cdot T_u$, $k \in \mathbb{N}_0 \equiv [0, 1, 2, \dots)$ and

$$\tau_k = |\mathrm{v}^d_k|;\ \mathrm{s}_k = \mathrm{Sign}\,\mathrm{v}^d_k;\ \mathrm{T}^d = \begin{cases} \mathrm{T}^d_+ & \mathrm{u}^n(\cdot) \neq 0, \\ \mathrm{T}^d_- & \mathrm{u}^n(\cdot) = 0; \end{cases}$$

$$\mathrm{u}^n(t, \tau_k, t_k) \equiv \begin{cases} 1 & t_k \le t < t_k + \phi(\cdot, \tau_k), \\ 0 & t_k + \phi(\cdot, \tau_k) \le t < t_{k+1}; \end{cases}$$

$$\phi(\tau_m, \tau^m, T_u, \tau_k) = \begin{cases} 0 & \tau_k < \tau_m; \\ \tau_k & \tau_m \le \tau_k < \tau^m; \\ \tau^m & \tau^m \le \tau_k < T_u; \\ T_u & \tau_k \ge T_u. \end{cases}$$

The description (4) is used for modelling the control torque vector $\mathbf{M}^{do}_o(t) = \{\mathrm{M}^{do}_i(t)\}$ of the attitude RT set at the PWM mode for their thrust control on a discrete command vector $\mathbf{v}^d_k = \{\mathrm{v}^d_{ik}\}$.

The GW precession model have the form

$$\mathrm{H} \begin{bmatrix} 0 & -C_\alpha \\ C_\alpha & 0 \end{bmatrix} \begin{bmatrix} \dot\beta \\ \dot\alpha \end{bmatrix} - \mathrm{H}\,\mathbf{A}^{\mathrm{t}}_{\mathrm{h}}\,\boldsymbol{\omega} = \begin{bmatrix} \mathrm{Q}'_\beta \\ \mathrm{Q}_\alpha \end{bmatrix}; \tag{5}$$

$$C^r\,\mathbf{h}^{\mathrm{t}}_{\mathrm{g}}(\alpha, \beta) \cdot \dot{\boldsymbol{\omega}} + \dot{\mathrm{H}} = \mathrm{Q}_r, \tag{6}$$

where C^r is the GW rotor moment of inertia, $\mathrm{Q}'_\beta \equiv \mathrm{Q}_\beta + S_\alpha\,\mathrm{Q}_r$, and $\mathrm{Q}_\nu \equiv \mathrm{M}_\nu - \mathrm{M}^{\mathrm{f}}_\nu$, $\nu = \beta, \alpha, r$ are generalized forces with the controlling M_ν and dry friction $\mathrm{M}^{\mathrm{f}}_\nu$ torques. The GW model of its motion on gimbal axes (5) have most cross-ratio

$$\begin{aligned} \dot\beta &= \ (\mathrm{M}_\alpha - \mathrm{Frk}_\alpha - \mathrm{M}^\omega_\alpha)/(\mathrm{H}\,C_\alpha); \\ \dot\alpha &= -(\mathrm{M}_\beta - \mathrm{Frk}_\beta - \mathrm{M}^\omega_\beta)/(\mathrm{H}\,C_\alpha) \end{aligned} \tag{7}$$

with the notations for $\nu = \alpha, \beta$: $\zeta_\nu = \mathrm{M}_\nu - \mathrm{M}^\omega_\nu$; $\mathrm{M}^\omega_\alpha = \mathrm{H}(\omega_\beta\,S_\alpha + \omega_y\,C_\alpha)$; $\mathrm{M}^\omega_\beta = \dot{\mathrm{H}}\,S_\alpha - \mathrm{H}\,\omega_\alpha\,C_\alpha$; $\omega_\alpha \equiv \omega_x C_\beta - \omega_z S_\beta$; $\omega_\beta \equiv \omega_x S_\beta + \omega_z C_\beta$ and

$$\mathrm{Frk}_\nu \equiv \mathrm{Frk}\,(\mathrm{M}^{\mathrm{fo}}_\nu, \dot\nu, \zeta_\nu) = \begin{cases} \mathrm{M}^{\mathrm{fo}}_\nu \cdot \mathrm{Sign}\,\dot\nu & \dot\nu \neq 0; \\ \mathrm{Sat}\,(\mathrm{M}^{\mathrm{fo}}_\nu, \zeta_\nu) & \dot\nu = 0, \end{cases}$$

where $\mathrm{M}^{\mathrm{fo}}_\nu > 0$ is value of a dry friction torque. At some time moments t_ν of a GW steady-state when $\dot\nu = 0$ for $\nu = \alpha \vee \beta$, a *principle problem* consists in determination of value M_ν for certain value M^ω_ν from *nonlinear set-valued* algebraic equation

$$\mathrm{M}_\nu - \mathrm{M}^\omega_\nu = \mathrm{Sat}\,(\mathrm{M}^{\mathrm{fo}}_\nu, \mathrm{M}_\nu - \mathrm{M}^\omega_\nu).$$

New method for extension of definition by the GW precession model (5) at such time moments was developed, its correctness was verified by results at both land-based and flight tests. At an input discrete signal x_k the holder model has the form: $\mathrm{Zh}[x_k, T_u] = x_k\ \forall t \in [t_k, t_k + T_u)$. The discrete control signals $\mathrm{u}^d_{\nu k}, \nu = \alpha, \beta$ lead to the gear output control torques M_ν taking into account the gear backlash d_ν and flexibility k_ν:

$$\mathrm{M}_\nu(t) = \mathrm{Satd}(\mathrm{M}^{\mathrm{m}}_\nu, b^\nu_{\mathrm{m}}, k_\nu, \delta\nu(t)), \tag{8}$$

where $\delta\nu(t) = \nu^{\mathrm{g}}(t) - \nu(t)$; $\nu^{\mathrm{g}}(t) = \mathrm{Zh}[\mathrm{u}^d_{\nu k}, T_u]$; $b^\nu_{\mathrm{m}} \equiv d_\nu/2$ and for $b^{\mathrm{m}}_\nu \equiv \mathrm{M}^{\mathrm{m}}_\nu/k_\nu - b^\nu_{\mathrm{m}}$ the function

$$\mathrm{Satd}(\cdot, x) \equiv \begin{cases} 0 & |x| \le b^\nu_{\mathrm{m}}; \\ k_\nu(x - b^\nu_{\mathrm{m}}\mathrm{Sign}\,x) & b^\nu_{\mathrm{m}} < |x| \le b^{\mathrm{m}}_\nu; \\ \mathrm{M}^{\mathrm{m}}_\nu\ \mathrm{Sign}\ x & |x| > b^{\mathrm{m}}_\nu. \end{cases}$$

Model of the control torque $\mathrm{M}_r(t)$ have the form

$$\mathrm{T}^{\mathrm{h}}_r\,\dot{\mathrm{M}}_r + \mathrm{M}_r = \mathrm{Sat}(\mathrm{M}^{\mathrm{m}}_r, k_r\,\mathrm{Zh}[\mathrm{u}^d_{rk}, T_u]) - b^{\mathrm{h}}_r \mathrm{H}. \tag{9}$$

The SAP driver model for a digital input $\dot\gamma^{pd}_k$ with some simplifying assumptions has the form $\dot\gamma^p(t) = \mathrm{Zh}[\dot\gamma^{pd}_k, T_u]$, moreover the $\ddot\gamma^p(t)$ modelling is effected by an impulse function.

3.4 Onboard Diagnostics and Reconfiguration

The *Sesat* ADCS diagnostics is carried out automatically by the onboard computer. The diagnosis algorithms are different for the ADCS modes. At TASM the *logic* reconfiguration algorithms are fulfilled by onboard computer basing on the diagnosis results, in addition a change of the applied onboard composition is possible by the Flight Control Center commands.

3.5 Properties of Spacecraft Flexible Structure

Contemporary computer-aided methods were applied for modelling the *Sesat* large-scale flexible SAPs, by 10 lower modes for each panel. Own dynamic properties of the *Sesat* flexible structure were carefully investigated by both spectral and frequency methods taking into account its parametric uncertainty and a panel angle $\gamma^p \in [0, 2\pi]$. These properties were also studied for its out-loop control by both the RT with the PWM and the GW at digital type, see Fig. 4, where the absolute pseudo-frequency $\lambda = (2/T_u)\mathrm{tg}(\omega T_u/2)$.

3.6 Synthesis of Observers and Control Laws

The synthesis of discrete observers and control laws at all ADCS modes was carried out by association of the *exact*

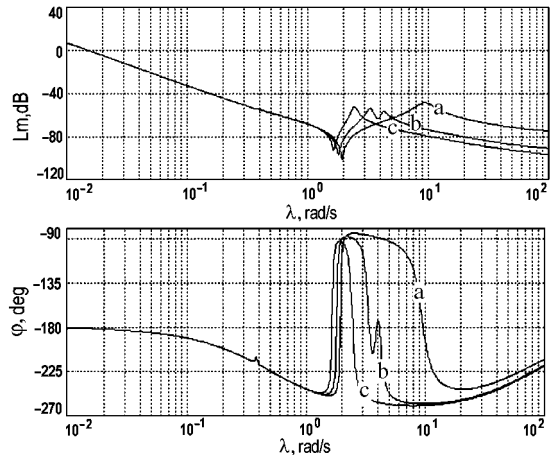

Fig. 4. Frequency characteristics on pitch channel: a) $\gamma^p = 0$; b) $\gamma^p = \pi/4$; c) $\gamma^p = \pi/2$

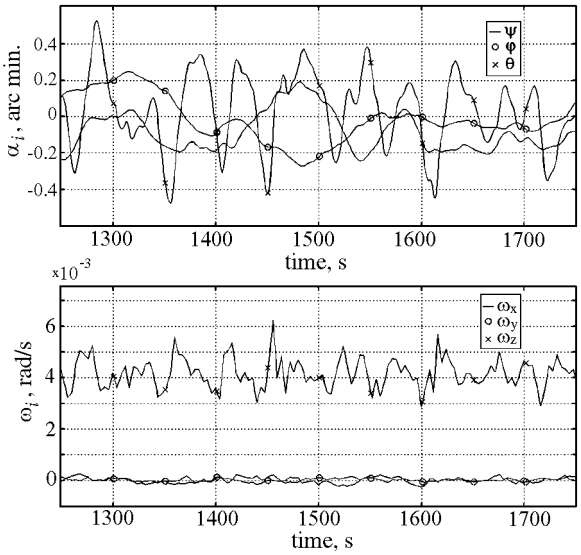

Fig. 5. The *Sesat* body orbital stabilization in TASM nominal sub-mode by the GU and GW

feedback linearization method and *vector Lyapunov function* (VLF) method. Let T_u and $T_q \le T_u$ are fixed *multiplicity* sampling periods of control and state measurement, and $x_k = x(t_k)$; $t_k = k\,T_u$; $t_s = s\,T_q$; $x_k^{\rm f} = \boldsymbol{\mathcal{F}}_{{\rm T}_u}(x_s)$, where $x_k^{\rm f}$ is a value of the variable x_s measured with the sampling period T_q, which is filtered out at the time $t = t_k$, and $\boldsymbol{\mathcal{F}}_{{\rm T}_u}(\cdot)$ is the *digital* filtering operator with the sampling period T_u.

Control in Initial Orientation Modes:

- at the DM: $\mathrm{v}_{ik}^d = k_p \cdot k_i^{\omega}\,(\omega_i^{\rm c} - \omega_{ik}^{\rm f}), i = x, y, z$, where k_p is an adjusted coefficient and vector $\boldsymbol{\omega}^{\rm c} = \{\omega_i^{\rm c}\}$ is given constant command;
- at SAM the following measured and *digitally* filtered variables are applied: $\boldsymbol{\omega}_k^{\rm f}$; $\alpha_{{\rm S}k}^{\rm f}$ and $\beta_{{\rm S}k}^{\rm f}$ with a computing the vector $\mathbf{S}_k^{\rm f}$ (Fig. 3) and the single-axis error vector $\boldsymbol{\varepsilon}_{{\rm S}k} = \mathbf{b}_y' \times \mathbf{S}_k^{\rm f}$;
- at the EAM and the EOPM, in addition to the SAM, the variables $\alpha_{ek}^{\rm f}$ and $\beta_{ek}^{\rm f}$ are used with a computing the vector $\mathbf{E}_k^{\rm f}$ (see Fig. 3), moreover also a command discrete signal on the Sun declination is applied.

Observers and Control Laws in the EOM are *nonlinear* and use only the following digitally filtered variables: $\alpha_{ek}^{\rm f}, \beta_{ek}^{\rm f}$ and $\mathrm{H}_k^{\rm f}, \alpha_k^{\rm f}, \beta_k^{\rm f}$.

Observers and Control Laws in the TASM are also *nonlinear.* At first in addition to the EOM a computed discrete value ψ_k^{sd} is applied in discrete observer basing on the filtered variables $\alpha_{{\rm S}k}^{\rm f}$ and $\beta_{{\rm S}k}^{\rm f}$ obtained by the fine digital Sun sensor. Then in nominal TASM sub-mode only the command values $\psi_k^{\rm c}, \varphi_k^{\rm c}, \theta_k^{\rm c}$ for the *Sesat* orbital attitude angels, the GU output filtered signals $\psi_k^{\rm gf}, \varphi_k^{\rm gf}, \theta_k^{\rm gf}$ and the GW filtered values $\beta_k^{\rm f}, \alpha_k^{\rm f}$ are applied in discrete observers and control laws.

3.7 Analysis and Computer Simulation

Applied *linear* methods for dynamic analysis are based on original theoretical results for general multiple continuous-discrete control systems with the different delays at a partial discrete measurement of the state vector and a physical forming control both on the PWM and digital type. The VLF method was used for a rigorous *nonlinear stability analysis* of the *Sesat* ADCS model (2) – (9) at all modes. The *Sesat* ADCS operation has been carefully simulated at all modes as well as all kind of their switching for a wide range of logic conditions, see Fig. 5.

4. THE OBSERVATION SATELLITE

The dynamic requirements to the attitude control systems (ACSs) for remote sensing spacecraft (SC) are:

- guidance the telescope's line-of-sight to a predetermined part of the Earth surface with the scan in designated direction;
- stabilization of an image motion at the onboard optical telescope focal plane.

Moreover, these requirements are expressed by rapid angular manoeuvering and spatial compensative motion with a variable vector of angular rate. Increased requirements to such information satellites (lifetime up to 10 years, exactness of spatial rotation manoeuvers with effective damping the SC flexible structure oscillations, robustness, fault-tolerance as well as to reasonable mass, size and energy characteristics) have motivated intensive development the gyro moment clusters (GMCs) based on excessive number of gyrodines (GDs) — single-gimbal control moment gyros.

4.1 Mathematical models

We introduce the inertial reference frame (IRF) $\mathbf{I}_{\oplus}$ ($\mathrm{O}_{\oplus}\mathrm{X}_{\rm e}^{\rm I}\mathrm{Y}_{\rm e}^{\rm I}\mathrm{Z}_{\rm e}^{\rm I}$), the geodesic Greenwich reference frame (GRF) $\mathbf{E}_{\rm e}$ ($\mathrm{O}_{\oplus}\mathrm{X}^{\rm e}\mathrm{Y}^{\rm e}\mathrm{Z}^{\rm e}$) which is rotated with respect to the IRF by angular rate vector $\boldsymbol{\omega}_{\oplus} \equiv \boldsymbol{\omega}_{\rm e}$ and the geodesic horizon reference frame (HRF) $\mathbf{E}_{\rm e}^{\rm h}$ ($\mathrm{C}\,\mathrm{X}_{\rm c}^{\rm h}\mathrm{Y}_{\rm c}^{\rm h}\mathrm{Z}_{\rm c}^{\rm h}$) with origin in a point C and ellipsoidal geodesic coordinates altitude H_c, longitude L_c and latitude B_c. There are standard defined the body reference frame (BRF) $\mathbf{B}$ ($\mathrm{O}xyz$) with origin in the SC mass center O, the orbit reference frame (ORF) $\mathbf{O}$ ($\mathrm{O}x^{\rm o}y^{\rm o}z^{\rm o}$), the optical telescope (sensor) reference frame (SRF) $\boldsymbol{\mathcal{S}}$ ($\mathrm{O}x^{\rm s}y^{\rm s}z^{\rm s}$) and the image field reference frame (FRF) $\boldsymbol{\mathcal{F}}$ ($\mathrm{O}_i x^i y^i z^i$) with origin in center O_i of the telescope focal plane $y^i\mathrm{O}_i z^i$. The BRF attitude with respect to the IRF is defined by quaternion

$\mathbf{\Lambda}_{\rm I}^{b} \equiv \mathbf{\Lambda} = (\lambda_0, \boldsymbol{\lambda}), \boldsymbol{\lambda} = (\lambda_1, \lambda_2, \lambda_3)$. Let us vectors $\boldsymbol{\omega}(t)$, $\mathbf{r}(t)$ and $\mathbf{v}(t)$ are standard denotations of the SC body vector angular rate, the SC mass center's position and progressive velocity with respect to the IRF. Further the symbols $\langle\cdot,\cdot\rangle$, $\times$, $\{\cdot\}$, $[\cdot]$ for vectors and $[\mathbf{a}\times]$, $(\cdot)^{\rm t}$ for matrixes are conventional denotations. The GMC's angular momentum (AM) vector $\boldsymbol{\mathcal{H}}$ have the form $\boldsymbol{\mathcal{H}}(\boldsymbol{\beta}) = {\rm h}_g \sum \mathbf{h}_p(\beta_p)$, there ${\rm h}_g$ is constant own AM value for each GD $p = 1, \dots m \equiv 1 \div m$ with the GD's AM unit $\mathbf{h}_p(\beta_p)$ and vector-column $\boldsymbol{\beta} = \{\beta_p\}$. Within precession theory of the control moment gyros, for a fixed position of the SC flexible structures with some simplifying assumptions and for $t \in {\rm T}_{t_0} = [t_0, +\infty)$ a SC angular motion model is appeared as

$$\dot{\mathbf{\Lambda}} = \mathbf{\Lambda} \circ \boldsymbol{\omega}/2; \quad \mathbf{A}^{o}\,\{\dot{\boldsymbol{\omega}}, \ddot{\mathbf{q}}\} = \{\mathbf{F}^{\omega}, \mathbf{F}^{q}\}, \qquad (10)$$

where $\boldsymbol{\omega} = \{\omega_i, i = x, y, z \equiv 1 \div 3\}$, $\mathbf{q} = \{q_j, j = 1 \div n^q\}$,

$$\mathbf{F}^{\omega} = \mathbf{M}^{\rm g} - \boldsymbol{\omega} \times \mathbf{G} + \mathbf{M}_d^{o}(t, \mathbf{\Lambda}, \boldsymbol{\omega}) + \mathbf{Q}^{o}(\boldsymbol{\omega}, \dot{\mathbf{q}}, \mathbf{q});$$

$$\mathbf{F}^{q} = \{-((\delta^q/\pi)\Omega_j^q \dot{q}_j + (\Omega_j^q)^2 q_j) + {\rm Q}_j^q(\boldsymbol{\omega}, \dot{q}_j, q_j)\};$$

$$\mathbf{A}^{o} = \begin{bmatrix} \mathbf{J} & \mathbf{D}_q \\ \mathbf{D}_q^{\rm t} & \mathbf{I} \end{bmatrix}; \; \begin{array}{l} \mathbf{G} = \mathbf{G}^{o} + \mathbf{D}_q \dot{\mathbf{q}}; \mathbf{M}^{\mathbf{g}} = -\dot{\boldsymbol{\mathcal{H}}} = -h_g \mathbf{A}_{\rm h}(\boldsymbol{\beta}) \ddot{\boldsymbol{\beta}}; \\ \mathbf{G}^{o} = \mathbf{J}\,\boldsymbol{\omega} + \boldsymbol{\mathcal{H}}(\boldsymbol{\beta}); \; \mathbf{A}_{\rm h}(\boldsymbol{\beta}) = \partial \mathbf{h}(\boldsymbol{\beta})/\partial \boldsymbol{\beta}, \end{array}$$

vector-column $\mathbf{M}_d^{o}(\cdot)$ presents an external torque disturbance, and $\mathbf{Q}^{o}(\cdot)$, ${\rm Q}_j^q(\cdot)$ are nonlinear continuous functions.

The GMC torque vector $\mathbf{M}^{\mathbf{g}}$ is presented as follows:

$$\mathbf{M}^{\mathbf{g}} = \mathbf{M}^{\mathbf{g}}(\boldsymbol{\beta}, \dot{\boldsymbol{\beta}}) = -\dot{\boldsymbol{\mathcal{H}}} = -h_g \mathbf{A}_{\rm h}(\boldsymbol{\beta})\, \mathbf{u}^{\rm g}; \quad \dot{\boldsymbol{\beta}} = \mathbf{u}^{\rm g}. \qquad (11)$$

Here $\mathbf{u}^{\rm g} = \{{\rm u}_p^{\rm g}\}$, ${\rm u}_p^{\rm g}(t) = a^{\rm g}\,{\rm Zh}[{\rm Sat}({\rm Qntr}(u_{pk}^g, d^g), \bar{\rm u}_{\rm g}^{\rm m}), T_u]$ with constants $a^{\rm g}$, d^g, $\bar{\rm u}_{\rm g}^{\rm m}$ and a control period $T_u = t_{k+1} - t_k$, $k \in \mathbb{N}_0 \equiv [0, 1, 2, ...)$; discrete functions $u_{pk}^g \equiv u_p^g(t_k)$ are outputs of digital nonlinear control law (CL), and functions ${\rm Sat}(x, a)$ and ${\rm Qntr}(x, a)$ are general-usage ones, while the holder model with the period T_u is such: $y(t) = {\rm Zh}[x_k, T_u] = x_k \;\forall t \in [t_k, t_{k+1})$.

At given the SC body angular programmed motion $\mathbf{\Lambda}^p(t)$, $\boldsymbol{\omega}^p(t)$, $\boldsymbol{\varepsilon}^p(t) = \dot{\boldsymbol{\omega}}^p(t)$ with respect to the IRF $\mathbf{I}_{\oplus}$ during time interval $t \in {\rm T} \equiv [t_{\rm i}, t_{\rm f}] \subset {\rm T}_{t_0}$, $t_{\rm f} \equiv t_{\rm i} + T$, and for forming the vector of corresponding continuous control torque $\mathbf{M}^{\mathbf{g}}(\boldsymbol{\beta}(t), \dot{\boldsymbol{\beta}}(t))$ (11), the vector-columns $\dot{\boldsymbol{\beta}} = \{\dot{\beta}_p\}$ and $\ddot{\boldsymbol{\beta}} = \{\ddot{\beta}_p\}$ must be component-wise module restricted:

$$|\dot{\beta}_p(t)| \le \bar{\rm u}_{\rm g} < \bar{\rm u}_{\rm g}^{\rm m}, \;\; |\ddot{\beta}_p(t)| \le \bar{\rm v}_{\rm g}, \; \forall t \in {\rm T}, \; p = 1 \div m, \; (12)$$

where values $\bar{\rm u}_{\rm g}$ and $\bar{\rm v}_{\rm g}$ are constant.

Collinear pair of two stopless GDs was named as *Scissored Pair Ensemble* (*SPE*) in well-known original work *J.W. Crenshaw* (1973). Redundant multiply scheme, based on six gyrodines in the form of three collinear GD's pairs, was named as *3-SPE*. Fig. 6 presents a simplest arrangement of this scheme into a canonical orthogonal gyroscopic basis $Ox_{\rm c}^{\rm g} y_{\rm c}^{\rm g} z_{\rm c}^{\rm g}$. By a slope of the GD pairs suspension axes in this basis it is possible to change essentially a form of the AM variation domain $\mathbf{S}$ at any direction. Based on four gyrodines the minimal redundant scheme *2-SPE* is easily obtained from the *3-SPE* scheme – without third pair (GD #5 and GD #6).

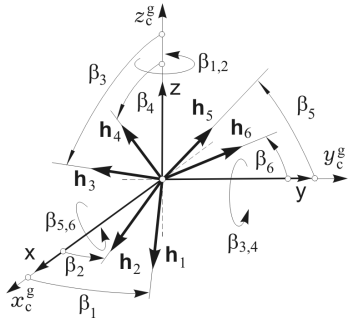

Fig. 6. The scheme *3-SPE*

In park state of above schemes one can have a vector of summary normed GMC's AM $\mathbf{h}(\boldsymbol{\beta}) \equiv \sum \mathbf{h}_p(\beta_p) = \mathbf{0}$.

4.2 The problem statement

Principle problem gets up on the SC angular guidance at a spatial course motion (SCM) when a space opto-electronic observation is executed at given time interval $t \in {\rm T}_n \equiv [t_{\rm i}^n, t_{\rm f}^n]$. This problem consists in determination of quaternion $\mathbf{\Lambda}(t)$ by the SC BRF $\mathbf{B}$ attitude with respect to the IRF $\mathbf{I}_{\oplus}$, angular rate vector $\boldsymbol{\omega}(t)$, vectors of angular acceleration $\boldsymbol{\varepsilon}(t)$ and its derivative $\dot{\boldsymbol{\varepsilon}}(t) = \boldsymbol{\varepsilon}^*(t) + \boldsymbol{\omega}(t) \times \boldsymbol{\varepsilon}(t)$ in the form of explicit functions, proceed from principle requirement: optical image of the Earth given part must to move by desired way at focal plane $y^i {\rm O}_i z^i$ of the telescope.

Into IRF the SC's spatial rotation maneuver (SRM) is described by kinematic relations

$$\dot{\mathbf{\Lambda}}(t) = \frac{1}{2} \mathbf{\Lambda} \circ \boldsymbol{\omega}(t); \; \dot{\boldsymbol{\omega}}(t) = \boldsymbol{\varepsilon}(t); \; \dot{\boldsymbol{\varepsilon}}(t) = \mathbf{v} \qquad (13)$$

during given time interval $t \in {\rm T}_p \equiv [t_{\rm i}^p, t_{\rm f}^p]$, $t_{\rm f}^p \equiv t_{\rm i}^p + T_p$. The optimization problem consists in determination of time functions $\mathbf{\Lambda}(t)$, $\boldsymbol{\omega}(t)$, $\boldsymbol{\varepsilon}(t)$ for the boundary conditions on left ($t = t_{\rm i}^p$) and right ($t = t_{\rm f}^p$) trajectory ends

$$\mathbf{\Lambda}(t_{\rm i}^p) = \mathbf{\Lambda}_{\rm i}; \; \boldsymbol{\omega}(t_{\rm i}^p) = \boldsymbol{\omega}_{\rm i}; \; \boldsymbol{\varepsilon}(t_{\rm i}^p) = \boldsymbol{\varepsilon}_{\rm i}; \qquad (14)$$

$$\mathbf{\Lambda}(t_{\rm f}^p) = \mathbf{\Lambda}_{\rm f}; \; \boldsymbol{\omega}(t_{\rm f}^p) = \boldsymbol{\omega}_{\rm f}; \; \boldsymbol{\varepsilon}(t_{\rm f}^p) = \boldsymbol{\varepsilon}_{\rm f} \qquad (15)$$

with optimization of the integral quadratic index

$$\mathrm{I}_{\rm o} = \frac{1}{2} \int_{t_{\rm i}^p}^{t_{\rm f}^p} \langle \mathbf{v}(\tau), \mathbf{v}(\tau) \rangle \, d\tau \Rightarrow \min. \qquad (16)$$

Onboard algorithms are needed for the SC guidance at a SRM taking into account the restrictions (12) to vectors $\dot{\boldsymbol{\beta}}(t)$ and $\ddot{\boldsymbol{\beta}}(t)$. Here for given time interval ${\rm T}_p$ a problem consists in determination the explicit time functions $\mathbf{\Lambda}(t)$, $\boldsymbol{\omega}(t)$, $\varepsilon(t)$ and $\dot{\boldsymbol{\varepsilon}}(t)$ for the boundary conditions (14), (15) and also for given condition

$$\dot{\boldsymbol{\varepsilon}}(t_{\rm f}^p) = \dot{\boldsymbol{\varepsilon}}_{\rm f} \equiv \boldsymbol{\varepsilon}_{\rm f}^* + \boldsymbol{\omega}_{\rm f} \times \boldsymbol{\varepsilon}_{\rm f}, \qquad (17)$$

which presents requirements to a *smooth conjugation* of guidance by a SRM with guidance at next the SC SCM.

Applied onboard measuring subsystem is based on inertial gyro unit corrected by the fine fixed-head star trackers. Contemporary filtering & alignment calibration algorithms give finally a fine discrete estimating the SC angular motion coordinates by the quaternion $\mathbf{\Lambda}_s^{\rm m} = \mathbf{\Lambda}_s \circ \mathbf{\Lambda}_s^{\rm n}$, $s \in \mathbb{N}_0$, where $\mathbf{\Lambda}_s \equiv \mathbf{\Lambda}(t_s)$, $\mathbf{\Lambda}_s^{\rm n}$ is a "noise-drift" digital quaternion and a measurement period $T_q = t_{s+1} - t_s \le T_u$ is multiply with respect to a control period T_u.

At a land-survey SC lifetime up to 5 years its structure inertial and flexible characteristics are slowly changed in wide boundaries, the solar array panels are rotated with respect to the SC body and the communication antennas are pointing for information service. Therefore inertial matrix $\mathbf{A}^{\rm o}$ (10) and partial frequencies Ω_j^q of the SC structure are not complete certain. Problems consist in synthesis of the SC guidance laws at its both the SCM and the SRM, and also in dynamical designing the GMC's robust digital control law $\mathbf{u}_k^g = \{u_{pk}^g\}$ on the quaternion values $\mathbf{\Lambda}_s^{\rm m}$ when the SC structure characteristics are uncertain and its damping is very weak, decrement of the SC structure oscillations $\delta_j^q \approx 5 \cdot 10^{-3}$ in (10).

4.3 Guidance at a course motion

Analytic matching solution have been obtained for problem of the SC angular guidance at the SCM at given time interval $t \in \mathrm{T}_n$. The solution is based on a vector composition of all elemental motions in the GRF $\mathbf{E}_\mathrm{e}$ using next reference frames: the HRF $\mathbf{E}^\mathrm{h}_\mathrm{e}$, the SRF $\boldsymbol{\mathcal{S}}$ and the FRF $\boldsymbol{\mathcal{F}}$. Vectors $\mathbf{r}(t)$ and $\mathbf{v}(t)$ are presented in the GRF $\mathbf{E}_\mathrm{e}$ as $\mathbf{r}^\mathrm{e} = \mathbf{T}^\mathrm{e}_\mathrm{I}\,\mathbf{r}$ and $\mathbf{v}^\mathrm{e} = \mathbf{T}^\mathrm{e}_\mathrm{I}\,(\mathbf{v} - [\omega_\oplus \mathbf{i}_3 \times]\mathbf{r}_\mathrm{o})$, $\mathbf{T}^\mathrm{e}_\mathrm{I} = [\rho_\mathrm{e}(t)]_3$ and $\rho_\mathrm{e}(t) = \rho^\mathrm{i}_\mathrm{e} + \omega_\oplus(t - t_\mathrm{i})$. Vectors $\boldsymbol{\omega}^\mathrm{s}_\mathrm{e}$ and $\mathbf{v}^\mathrm{s}_\mathrm{e}$ are defined as

$$\boldsymbol{\omega}^\mathrm{s}_\mathrm{e} = \{\omega^\mathrm{s}_{\mathrm{e}i}\} = \mathbf{T}^\mathrm{s}_b(\boldsymbol{\omega} - \tilde{\boldsymbol{\Lambda}} \circ \omega_\oplus \mathbf{i}_3 \circ \boldsymbol{\Lambda});\ \mathbf{v}^\mathrm{s}_\mathrm{e} = \tilde{\boldsymbol{\Lambda}}^\mathrm{s}_\mathrm{e} \circ \mathbf{v}^\mathrm{e}_\mathrm{o} \circ \boldsymbol{\Lambda}^\mathrm{s}_\mathrm{e},$$

where $\boldsymbol{\Lambda} = \boldsymbol{\Lambda}^b_\mathrm{I}; \boldsymbol{\Lambda}^\mathrm{s}_\mathrm{e} = \boldsymbol{\Lambda}^\mathrm{I}_\mathrm{e} \circ \boldsymbol{\Lambda}^b_\mathrm{I} \circ \boldsymbol{\Lambda}^\mathrm{s}_b$, $\dot{\boldsymbol{\Lambda}}^\mathrm{s}_\mathrm{e} = \boldsymbol{\Lambda}^\mathrm{s}_\mathrm{e} \circ \boldsymbol{\omega}^\mathrm{s}_\mathrm{e}/2$, and constant matrix $\mathbf{T}^\mathrm{s}_b$ represents the telescope fixation on the SC body. For any observed point C the oblique range D is analytically calculated as $\mathrm{D} = |\mathbf{r}^\mathrm{e}_\mathrm{c} - \mathbf{r}^\mathrm{e}|$. If orthogonal matrix $\mathbf{C}^\mathrm{s}_\mathrm{h} \equiv \tilde{\mathbf{C}} = \|\tilde{c}_{ij}\|$ defines the SRF $\boldsymbol{\mathcal{S}}$ attitude with respect to the HRF $\mathbf{E}^\mathrm{h}_\mathrm{e}$, then for any point $\mathrm{M}(\tilde{y}^i, \tilde{z}^i)$ at the telescope focal plane $y^i \mathrm{O}_i z^i$ the components $\tilde{V}^i_y$ and $\tilde{V}^i_z$ of normed vector by an image motion velocity is appeared as

$$\begin{bmatrix} \tilde{V}^i_y \\ \tilde{V}^i_z \end{bmatrix} \equiv \begin{bmatrix} \dot{\tilde{y}}^i \\ \dot{\tilde{z}}^i \end{bmatrix} = \begin{bmatrix} \tilde{y}^i & 1 & 0 \\ \tilde{z}^i & 0 & 1 \end{bmatrix} \begin{bmatrix} q^i \tilde{\mathrm{v}}^\mathrm{s}_{\mathrm{e}1} - \tilde{y}^i\ \omega^\mathrm{s}_{\mathrm{e}3} + \tilde{z}^i\ \omega^\mathrm{s}_{\mathrm{e}2} \\ q^i \tilde{\mathrm{v}}^\mathrm{s}_{\mathrm{e}2} - \quad \omega^\mathrm{s}_{\mathrm{e}3} - \tilde{z}^i\ \omega^\mathrm{s}_{\mathrm{e}1} \\ q^i \tilde{\mathrm{v}}^\mathrm{s}_{\mathrm{e}3} + \quad \omega^\mathrm{s}_{\mathrm{e}2} + \tilde{y}^i\ \omega^\mathrm{s}_{\mathrm{e}1} \end{bmatrix}. \quad (18)$$

Here normed focal coordinates $\tilde{y}^i = y^i/f_e$ and $\tilde{z}^i = z^i/f_e$, where f_e is the telescope equivalent focal distance; function $q^i \equiv 1 - (\tilde{c}_{21}\tilde{y}^i + \tilde{c}_{31}\tilde{z}^i)/\tilde{c}_{11}$, and vector of normed SC's mass center velocity have the components $\tilde{\mathrm{v}}^\mathrm{s}_{\mathrm{e}i} = \mathrm{v}^\mathrm{s}_{\mathrm{e}i}/\mathrm{D}, i = 1 \div 3$. For given image velocity $\tilde{\mathrm{W}}^s_y = \mathrm{const}$ and conditions

$$\tilde{V}^i_y(0,0) = \tilde{\mathrm{W}}^i_y = -\tilde{\mathrm{W}}^s_y;\ \tilde{V}^i_z(0,0) = 0;\ \partial \tilde{V}^i_y(0,0)/\partial \tilde{z}^i = 0$$

calculation of vector $\boldsymbol{\omega}^\mathrm{s}_\mathrm{e}$ is carried out by the relations

$$\omega^\mathrm{s}_{\mathrm{e}1} = -\tilde{\mathrm{v}}^\mathrm{s}_{\mathrm{e}2}\tilde{c}_{31}/\tilde{c}_{11};\ \omega^\mathrm{s}_{\mathrm{e}2} = -\tilde{\mathrm{v}}^\mathrm{s}_{\mathrm{e}3};\ \omega^\mathrm{s}_{\mathrm{e}3} = -\tilde{W}^i_y + \tilde{\mathrm{v}}^\mathrm{s}_{\mathrm{e}2}. \quad (19)$$

By numerical solution of the quaternion differential equation $\dot{\boldsymbol{\Lambda}}^\mathrm{s}_\mathrm{e} = \boldsymbol{\Lambda}^\mathrm{s}_\mathrm{e} \circ \boldsymbol{\omega}^\mathrm{s}_\mathrm{e}/2$ with regard to (19) one can obtain values $\boldsymbol{\lambda}^\mathrm{s}_{\mathrm{e}s} \equiv \boldsymbol{\lambda}^\mathrm{s}_\mathrm{e}(t_s)$ for the discrete time moments $t_s \in \mathrm{T}_n$ with period T_q, $s = 0 \div n_q$, $n_q = T_n/T_q$ when initial value $\boldsymbol{\Lambda}^\mathrm{s}_\mathrm{e}(t^n_\mathrm{i})$ is given. Further solution is based on the elegant extrapolation of values $\boldsymbol{\sigma}^\mathrm{s}_{\mathrm{e}s} = \boldsymbol{\lambda}^\mathrm{s}_{\mathrm{e}s}/(1 + \lambda^\mathrm{s}_{0\,\mathrm{e}s})$ by the vector of Rodrigues' modified parameters and values $\boldsymbol{\omega}^\mathrm{s}_{\mathrm{e}s}$ by the angular rate vector. The extrapolation is carried out by two sets of n_q coordinated 3-degree vector splines with analytical obtaining a high-precise approximation of the SRF $\boldsymbol{\mathcal{S}}$ guidance motion with respect to the GRF $\mathbf{E}_\mathrm{e}$ both on vector of angular acceleration and on vector of its local derivative. At last stage, required functions $\boldsymbol{\Lambda}(t), \boldsymbol{\omega}(t), \boldsymbol{\varepsilon}(t)$ and $\dot{\boldsymbol{\varepsilon}}(t) = \boldsymbol{\varepsilon}^*(t) + \boldsymbol{\omega}(t) \times \boldsymbol{\varepsilon}(t)$ is calculated by *explicit* formulas. These functions are applied at onboard computer for the time moments $t_s \in \mathrm{T}_n$, and also for calculation (18) of the image velocity at any point $\mathrm{M}(\tilde{y}^i, \tilde{z}^i)$ into the telescope focal plane for any $t \in \mathrm{T}_n$.

4.4 Optimization of a rotation maneuver

Optimal one-axis problem is very simple, the SC optimal motion with respect to any k axis is presented by the analytic function $\varphi_k(t)$ in a class of the five degree polynomials (splines) by normed time $\tau = (t - t^p_\mathrm{i})/T_p \subset [0, 1]$.

Developed analytical approach to the problem is based on necessary and sufficient condition for solvability of Darboux problem. At general case the solution is presented as result of composition by three ($k = 1 \div 3$) simultaneously derived elementary rotations of embedded bases $\mathbf{E}_k$ about units $\mathbf{e}_k$ of Euler axes, which positions are defined from the boundary conditions (15) and (16) for initial spatial problem. For all 3 elementary rotations with respect to units $\mathbf{e}_k$ the boundary conditions are analytically assigned. Into the IRF $\mathbf{I}_\oplus$ the quaternion $\boldsymbol{\Lambda}(t)$ is defined by the production

$$\boldsymbol{\Lambda}(t) = \boldsymbol{\Lambda}_\mathrm{i} \circ \boldsymbol{\Lambda}_1(t) \circ \boldsymbol{\Lambda}_2(t) \circ \boldsymbol{\Lambda}_3(t), \quad (20)$$

where $\boldsymbol{\Lambda}_k(t) = (\cos(\varphi_k(t)/2), \sin(\varphi_k(t)/2)\mathbf{e}_k)$, and functions $\varphi_k(t)$ analytically present the elementary rotation angles. Let the quaternion $\boldsymbol{\Lambda}^* \equiv (\lambda^*_0, \boldsymbol{\lambda}^*) = \tilde{\boldsymbol{\Lambda}}_\mathrm{i} \circ \boldsymbol{\Lambda}_\mathrm{f} \neq \mathbf{1}$ have the Euler axis unit $\mathbf{e}_3 = \boldsymbol{\lambda}^*/\sin(\varphi^*/2)$ by 3-rd elementary rotation, where angle $\varphi^* = 2\arccos(\lambda^*_0)$. For elementary rotations there are applied the boundary quaternions:

$$\begin{aligned} &\boldsymbol{\Lambda}_1(t^p_\mathrm{i}) = \boldsymbol{\Lambda}_1(t^p_\mathrm{f}) = \boldsymbol{\Lambda}_2(t^p_\mathrm{i}) = \boldsymbol{\Lambda}_2(t^p_\mathrm{f}) = \boldsymbol{\Lambda}_3(t^p_\mathrm{i}) = \mathbf{1}; \\ &\boldsymbol{\Lambda}_3(t^p_\mathrm{f}) = (\cos(\varphi^\mathrm{f}_3/2), \mathbf{e}_3 \sin(\varphi^\mathrm{f}_3/2)), \end{aligned} \quad (21)$$

where $\varphi^\mathrm{f}_3 = \varphi^*$ and $\mathbf{1}$ is a single quaternion. Unit $\mathbf{e}_1$ of 1-st elementary rotation's Euler axis is selected by simple algorithm and then unit $\mathbf{e}_2$ is defined as $\mathbf{e}_2 = \mathbf{e}_3 \times \mathbf{e}_1$. All vectors $\boldsymbol{\omega}_k(t)$, $\boldsymbol{\varepsilon}_k(t)$ and $\dot{\boldsymbol{\varepsilon}}_k(t)$ have analytic form which is optimal on index (16) for each elementary rotation. Vectors $\boldsymbol{\omega}(t)$, $\boldsymbol{\varepsilon}(t)$ and $\dot{\boldsymbol{\varepsilon}}(t) \equiv \mathbf{v}(t)$ are analytically defined by recurrent algorithm using functions $\varphi_k(t)$ and their derivatives.

For nonlinear problem (13) – (16) Hamilton function

$$H = -\frac{1}{2}\langle \mathbf{v}, \mathbf{v} \rangle + \frac{1}{2}\langle \mathrm{vect}(\tilde{\boldsymbol{\Lambda}} \circ \boldsymbol{\Psi}), \boldsymbol{\omega} \rangle + \langle \boldsymbol{\mu}, \boldsymbol{\varepsilon} \rangle + \langle \boldsymbol{\nu}, \mathbf{v} \rangle$$

have associated variables – vectors $\boldsymbol{\mu}, \boldsymbol{\nu}$ and quaternion $\boldsymbol{\Psi} = \mathbf{C}_\varphi \circ \boldsymbol{\Lambda}$, where $\mathbf{C}_\varphi = (\mathrm{c}_{\varphi 0}, \mathbf{c}_\varphi)$ is the normed quaternion with a vector part $\mathbf{c}_\varphi = \{\mathrm{c}_{\varphi k}\}$. The associated differential system

$$\dot{\boldsymbol{\Psi}} = \frac{1}{2}\boldsymbol{\Psi} \circ \boldsymbol{\omega};\ \dot{\boldsymbol{\mu}} = -\frac{1}{2}\tilde{\boldsymbol{\Lambda}} \circ \mathbf{c}_\varphi \circ \boldsymbol{\Lambda};\ \dot{\boldsymbol{\nu}} = -\boldsymbol{\mu} \quad (22)$$

and the optimality condition $\partial H/\partial \mathbf{v} = -\mathbf{v} + \boldsymbol{\nu} = \mathbf{0}$ give the optimal " control "

$$\mathbf{v}(t) = \boldsymbol{\nu}(t) = \mathbf{c}_\varepsilon - \mathbf{c}_\omega(t - t^p_\mathrm{i}) + \frac{1}{2}\int_{t^p_\mathrm{i}}^{t}\left(\int_{t^p_\mathrm{i}}^{\tau} \tilde{\boldsymbol{\Lambda}}(s) \circ \mathbf{c}_\varphi \circ \boldsymbol{\Lambda}(s) ds\right) d\tau,$$

where vectors $\mathbf{c}_\varphi$, $\mathbf{c}_\omega = \{\mathrm{c}_{\omega k}\}$ and $\mathbf{c}_\varepsilon = \{\mathrm{c}_{\varepsilon k}\}$ must be numerically defined using known analytical structure of solution for direct system (13) and taking into account the boundary conditions (14) and (15). Standard Newton iteration method was applied for numerical obtaining a strict optimal "control" $\mathbf{v}(t)$, moreover analytical solution (initial point) was applied in the form of approximate optimal motion (20) and (21). Difference between approximate optimal motion and strict optimal motion is very light for the SC practical rotational maneuvers.

4.5 Guidance at a rotation maneuver

Fast onboard algorithms for the SC guidance at a SRM with restrictions to $\boldsymbol{\omega}(t)$, $\boldsymbol{\varepsilon}(t)$, $\dot{\boldsymbol{\varepsilon}}(t)$, corresponding restrictions to $\mathbf{h}(\boldsymbol{\beta}(t)), \dot{\boldsymbol{\beta}}(t)$ and $\ddot{\boldsymbol{\beta}}(t)$ in a class of the SC angular motions, were elaborated. Developed analytical approach to the problem is based on approximate optimal motion (20), (20) with boundary conditions (14), (15) and (17). Here functions $\varphi_k(t)$ are selected in a class of splines by five and six degree, moreover a module of a angular rate $\dot{\varphi}_3(t)$ in a position transfer ($k = 3$) may be limited when functions $\dot{\varphi}_1(t) = \dot{\varphi}_2(t) \equiv 0$. The technique is based on

the generalized integral's properties for the AM of the mechanical system "SC+GMC" and allows to evaluate vectors $\boldsymbol{\beta}(t)$, $\dot{\boldsymbol{\beta}}(t)$, $\ddot{\boldsymbol{\beta}}(t)$ in analytical form for a preassigned SC motion $\boldsymbol{\Lambda}(t)$, $\boldsymbol{\omega}(t)$, $\boldsymbol{\varepsilon}(t)$, $\dot{\boldsymbol{\varepsilon}}(t)\,\forall t \in \mathrm{T}_p$.

Into orthogonal canonical basis Oxyz, see Fig. 6, the GD's AM units have next projections:

$$x_1 = C_1;\ x_2 = C_2;\ y_1 = S_1;\ y_2 = S_2;\ x_3 = S_3;\ x_4 = S_4;$$
$$z_3 = C_3;\ z_4 = C_4;\ y_5 = C_5;\ y_6 = C_6;\ z_5 = S_5;\ z_6 = S_6,$$

where $S_p \equiv \sin\beta_p$ and $C_p \equiv \cos\beta_p$. Then vector-column $\mathbf{h}(\boldsymbol{\beta}) = \{\mathsf{x}, \mathsf{y}, \mathsf{z}\}$ of normed GMC's summary AM vector and matrix $\mathbf{A}_{\mathrm{h}}(\boldsymbol{\beta}) = \partial\mathbf{h}/\partial\boldsymbol{\beta}$ have the form

$$\mathbf{h}(\boldsymbol{\beta}) = \begin{bmatrix} \Sigma x_p \\ \Sigma y_p \\ \Sigma z_p \end{bmatrix}; \mathbf{A}_{\mathrm{h}}(\boldsymbol{\beta}) = \begin{bmatrix} -y_1 & -y_2 & z_3 & z_4 & 0 & 0 \\ x_1 & x_2 & 0 & 0 & -z_5 & -z_6 \\ 0 & 0 & -x_3 & -x_4 & y_5 & y_6 \end{bmatrix}.$$

For *3-SPE* scheme singular state is appeared when the matrix Gramme $\mathbf{G}(\boldsymbol{\beta}) = \mathbf{A}_h(\boldsymbol{\beta})\mathbf{A}_h^{\mathrm{t}}(\boldsymbol{\beta})$ loses its full rang, e.g. when $\mathsf{G} \equiv \det\mathbf{G}(\boldsymbol{\beta}) = 0$. At introducing the denotations

$$x_{12} = x_1 + x_2;\quad x_{34} = x_3 + x_4;\quad y_{12} = y_1 + y_2;$$
$$y_{56} = y_5 + y_6;\quad z_{34} = z_3 + z_4;\quad z_{56} = z_5 + z_6;$$
$$\tilde{x}_{12} = x_{12}/\sqrt{4 - y_{12}^2}\ ;\ \tilde{x}_{34} = x_{34}/\sqrt{4 - z_{34}^2};$$
$$\tilde{y}_{12} = y_{12}/\sqrt{4 - x_{12}^2}\ ;\ \tilde{y}_{56} = y_{56}/\sqrt{4 - z_{56}^2};$$
$$\tilde{z}_{34} = z_{34}/\sqrt{4 - x_{34}^2}\ ;\quad \tilde{z}_{56} = z_{56}/\sqrt{4 - y_{56}^2}$$

components of the GMC explicit vector tuning law

$$\mathbf{f}_\rho(\boldsymbol{\beta}) \equiv \{f_{\rho 1}(\boldsymbol{\beta}), f_{\rho 2}(\boldsymbol{\beta}), f_{\rho 3}(\boldsymbol{\beta})\} = \mathbf{0} \qquad (23)$$

are applied in the form

$$f_{\rho 1}(\boldsymbol{\beta}) \equiv \tilde{x}_{12} - \tilde{x}_{34} + \rho\ (\tilde{x}_{12}\ \tilde{x}_{34} - 1);$$
$$f_{\rho 2}(\boldsymbol{\beta}) \equiv \tilde{y}_{56} - \tilde{y}_{12} + \rho\ (\tilde{y}_{56}\ \tilde{y}_{12} - 1);$$
$$f_{\rho 3}(\boldsymbol{\beta}) \equiv \tilde{z}_{34} - \tilde{z}_{56} + \rho\ (\tilde{z}_{34}\ \tilde{z}_{56} - 1).$$

The analytical proof have been elaborated that vector tuning law (23) ensures absent of singular states by this GMC scheme for all values of the GMC AM vector $\mathbf{h}(t) \in \mathbf{S} \setminus \mathbf{S}^*$, i.e. inside all its variation domain. For the representation

$$x_{12} = (\mathsf{x} + \Delta_x)/2;\quad x_{34} = (\mathsf{x} - \Delta_x)/2;$$
$$y_{56} = (\mathsf{y} + \Delta_y)/2;\quad y_{12} = (\mathsf{y} - \Delta_y)/2;$$
$$z_{34} = (\mathsf{z} + \Delta_z)/2;\quad z_{56} = (\mathsf{z} - \Delta_z)/2$$

and the denotation $\boldsymbol{\Delta} = \{\Delta_x, \Delta_y, \Delta_z\}$ one can obtain the nonlinear vector equation $\boldsymbol{\Delta}(t) = \boldsymbol{\Phi}(\mathbf{h}(t), \boldsymbol{\Delta}(t))$. At a known vector $\mathbf{h}(t)$ this equation have single solution $\boldsymbol{\Delta}(t)$, which is readily computed by method of a simple iteration. Further the units $\mathbf{h}_p(\beta_p(t))$ and vector-columns $\boldsymbol{\beta}(t)$, $\dot{\boldsymbol{\beta}}(t)$, $\ddot{\boldsymbol{\beta}}(t)$ are calculated by the explicit analytical relations $\forall t \in \mathrm{T}_p$. For the *2-SPE* scheme such evaluation is carried out by the explicit analytical formulas only.

4.6 Filtering and digital control

In stage 1, for continuous forming the control torque $\mathbf{M}^{\mathbf{g}}(\boldsymbol{\beta}(t), \dot{\boldsymbol{\beta}}(t))$ (11) and the SC model as a free rigid body the simplified controlled object is such:

$$\dot{\boldsymbol{\Lambda}} = \boldsymbol{\Lambda} \circ \boldsymbol{\omega}/2;\quad \mathbf{J}\dot{\boldsymbol{\omega}} + [\boldsymbol{\omega}\times]\mathbf{G}^o = \mathbf{M}^{\mathbf{g}};\quad \dot{\boldsymbol{\beta}} = \mathbf{u}^{\mathrm{g}}(t). \qquad (24)$$

The error quaternion is $\mathbf{E} = (e_0, \mathbf{e}) = \tilde{\boldsymbol{\Lambda}}^p(t) \circ \boldsymbol{\Lambda}$, Euler parameters' vector is $\boldsymbol{\mathcal{E}} = \{e_0, \mathbf{e}\}$, and the attitude error's matrix is $\mathbf{C}_e \equiv \mathbf{C}(\boldsymbol{\mathcal{E}}) = \mathbf{I}_3 - 2[\mathbf{e}\times]\mathbf{Q}_e$, where $\mathbf{Q}_e \equiv \mathbf{Q}(\boldsymbol{\mathcal{E}}) = \mathbf{I}_3 e_0 + [\mathbf{e}\times]$ with $\det(\mathbf{Q}_e) = e_0$. If error $\delta\boldsymbol{\omega} \equiv \tilde{\boldsymbol{\omega}}$ in the rate vector $\boldsymbol{\omega}$ is defined as $\tilde{\boldsymbol{\omega}} = \boldsymbol{\omega} - \mathbf{C}_e\boldsymbol{\omega}^p(t)$, and the GMC's required control torque vector $\mathbf{M}^{\mathbf{g}}$ is formed as

$$\mathbf{M}^{\mathbf{g}} = \boldsymbol{\omega}\times\mathbf{G}^o + \mathbf{J}(\mathbf{C}_e\dot{\boldsymbol{\omega}}^p(t) - [\boldsymbol{\omega}\times]\mathbf{C}_e\boldsymbol{\omega}^p(t) + \tilde{\mathbf{m}}),$$

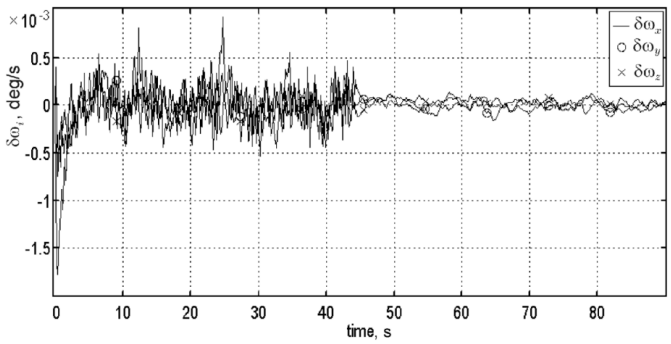

Fig. 7. Rate errors for consequence of the SRM and SCM

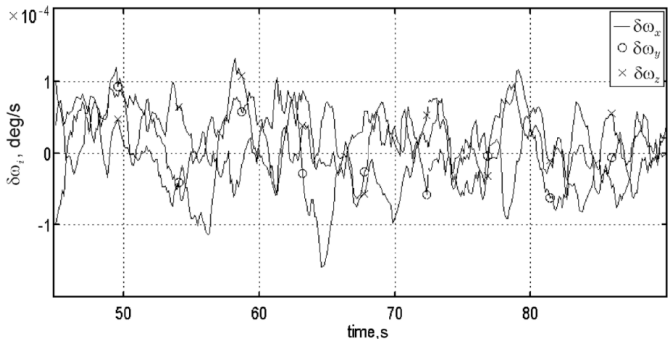

Fig. 8. The rate errors at the spatial course motion

then the simplest nonlinear model of the SC's attitude error is as follows:

$$\dot{e}_0 = -\langle \mathbf{e}, \tilde{\boldsymbol{\omega}}\rangle/2;\quad \dot{\mathbf{e}} = \mathbf{Q}_e\tilde{\boldsymbol{\omega}}/2;\quad \dot{\tilde{\boldsymbol{\omega}}} = \tilde{\mathbf{m}}. \qquad (25)$$

For model (25) a *non-local nonlinear* coordinate transformation is defined and applied at analytical synthesis by the EFL technique. This results in the nonlinear CL

$$\tilde{\mathbf{m}}(\boldsymbol{\mathcal{E}}, \tilde{\boldsymbol{\omega}}) = -\mathbf{A}_0\ \mathbf{e}\ \mathrm{sgn}(e_0) - \mathbf{A}_1\ \tilde{\boldsymbol{\omega}}, \qquad (26)$$

where $\mathbf{A}_0 = ((2a_0^* - \tilde{\omega}^2/2)/e_0)\mathbf{I}_3$; $\mathbf{A}_1 = a_1^*\mathbf{I}_3 - \mathbf{R}_{e\omega}$, $\mathrm{sgn}(e_0) = (1,\ \text{if}\ e_0 \geq 0) \vee (-1,\ \text{if}\ e_0 < 0)$, matrix $\mathbf{R}_{e\omega} = \langle \mathbf{e}, \tilde{\boldsymbol{\omega}}\rangle\mathbf{Q}_e^{\mathrm{t}}[\mathbf{e}\times]/(2e_0)$, and parameters a_0^*,a_1^* are analytically calculated on spectrum $\mathrm{S}_{ci}^* = -\alpha_c \pm j\omega_c$. Simultaneously the VFL $\boldsymbol{\upsilon}(\boldsymbol{\mathcal{E}}, \tilde{\boldsymbol{\omega}})$ is analytically constructed for close-loop system (25) and (26).

Discrete measured error quaternion and Euler parameters' vector are $\mathbf{E}_s = (e_{0s}, \mathbf{e}_s) = \tilde{\boldsymbol{\Lambda}}^p(t_s) \circ \boldsymbol{\Lambda}_s^{\mathrm{m}}$ and $\boldsymbol{\mathcal{E}}_s = \{e_{0s}, \mathbf{e}_s\}$, and the attitude error filtering is executed by the relations

$$\tilde{\mathbf{x}}_{s+1} = \tilde{\mathbf{A}}\tilde{\mathbf{x}}_s + \tilde{\mathbf{B}}\mathbf{e}_s; \mathbf{e}_s^{\mathrm{f}} = \tilde{\mathbf{C}}\tilde{\mathbf{x}}_s + \tilde{\mathbf{D}}\mathbf{e}_s, \qquad (27)$$

where matrices $\tilde{\mathbf{A}}, \tilde{\mathbf{B}}, \tilde{\mathbf{C}}$ and $\tilde{\mathbf{D}}$ have conforming dimensions and some general turning parameters. Attitude filtered error vector $\mathbf{e}_k^{\mathrm{f}}$ is applied for forming the digital control $\tilde{\mathbf{m}}_k = \mathbf{u}_k$ taking into account a time delay at incomplete measurement of state and onboard signal processing:

$$\mathbf{v}_k = -(\mathbf{K}_{\mathrm{d}}^{\mathrm{x}}\,\hat{\mathbf{x}}_k + \mathbf{K}_{\mathrm{d}}^{\mathrm{u}}\,\mathbf{u}_k);\quad \mathbf{u}_{k+1} = \mathbf{v}_k,\quad k \in \mathbb{N}_0; \qquad (28)$$
$$\hat{\mathbf{x}}_{k+1} = \mathbf{A}_{\mathrm{od}}\,\hat{\mathbf{x}}_k + \mathbf{B}_{\mathrm{od}}^{\mathrm{u}}\,\mathbf{u}_k + \mathbf{B}_{\mathrm{od}}^{\mathrm{v}}\,\mathbf{v}_k$$
$$+\mathbf{G}_{\mathrm{d}}(\mathbf{e}_k^{\mathrm{f}} - (\mathbf{C}_{\mathrm{od}}\,\hat{\mathbf{x}}_k + \mathbf{D}_{\mathrm{od}}^{\mathrm{u}}\,\mathbf{u}_k + \mathbf{D}_{\mathrm{od}}^{\mathrm{v}}\,\mathbf{v}_k)),$$

where $\hat{\mathbf{x}}_k = \{\hat{\mathbf{e}}_k, \hat{\tilde{\boldsymbol{\omega}}}_k\}$, matrices have conforming dimensions and also general turning parameters.

In stage 2, the problems of synthesising digital nonlinear CL were solved for model of the flexible spacecraft (10) with incomplete discrete measurement of state. Furthermore, the selection of parameters in the structure of the

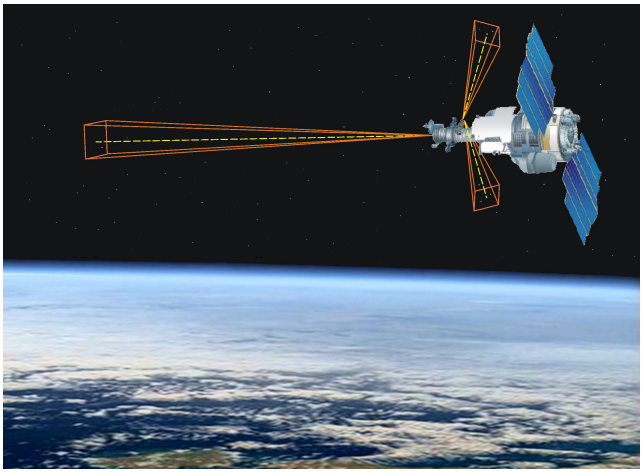

Fig. 9. Mode of astronomical checking axes' concordance

GMC nonlinear robust CL (which optimizes the main quality criterion for given restrictions, including coupling and damping the SC structure oscillations is fulfilled by a parametric optimization of the comparison system for the VLF and multistage numerical simulation. Thereto, the VLF has the structure derived above for the error coordinates $\boldsymbol{\mathcal{E}}, \tilde{\boldsymbol{\omega}}$ and the structure of other VLF components in the form of *sublinear norms* for vector variables $\mathbf{q}(t)$, $\dot{\mathbf{q}}(t)$, $\dot{\boldsymbol{\beta}}(t)$ using the vector $\boldsymbol{\beta}(t)$.

4.7 Computer simulation

Fig. 7 and Fig. 8 present some results on computer simulation of a gyromoment ACS for Russian remote sensing SC by the *Resource-DK* type. Here the rate errors are represented at consequence of the SC spatial rotational maneuver for time $t \in [0, 45)$ sec and the SC spatial course motion for time $t \in [45, 90]$ sec. Applied digital robust nonlinear control law is flexible switched at the time moment $t = 45$ sec on astatic ones with respect to the acceleration.

5. NEW CHALLENGES

5.1 Alignment calibration of the star trackers

The characteristics of pointing an orbital telescope's line-of-sight onto observed objects and quality of observation information being obtained are strongly dependent on the accuracy of defining the relative position of reference frames (RFs) connected with an orbital telescope (OT) and with the main measuring devices, namely, the star trackers (STs) used in the SC attitude control system. A special mode is organized for mutual binding these reference frames, when a telescope scans the star sky and simultaneously the optoelectronic STs' measurements are registered, see Fig. 9. The elaborated innovation methods for a more accurate definition of actual position of the OT and the star tracker cluster (STC) by a posterior processing of the measurement information directly aboard spacecraft, are presented.

The following problems are solved at the known coordinates of the SC mass center orbital motion:

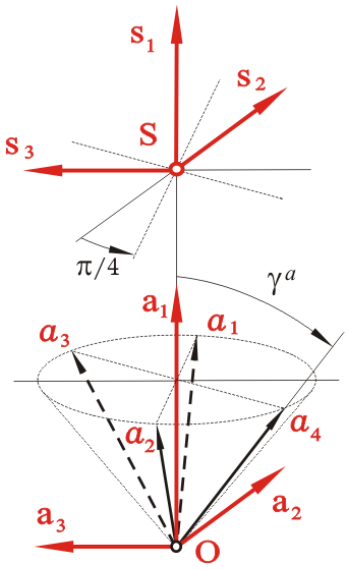

Fig. 10. The bases **S** and **A**

- definition of the angular position of the base **S** during a mode of astronomical checking axes' concordance (ACAC), when the measuring information only from a telescope is applied;
- definition of a fixed mutual angular position of the bases **A** and **S** (the alignment identification), when the measuring information obtained in the ACAC mode both from a telescope and star trackers is applied.

5.2 Smoothing the Discrete Measurements

Solution of practical tasks demonstrates that it is rational to apply method (filter) of the Savitsky – Goley polynomial smoothing that is a modification of the MLS. The problem on definition of the mutual attitude of two orthogonal bases on the basis of the data about two sets of units that are arbitrarily placed in the bases, is more complex. Let a set of the units $\mathbf{b}_i$ be given that are measured in the SC body base **B**, and a set of values of the units $\mathbf{r}_i$ corresponding to them specified in the inertial base **I**. The classical problem of vector matching (the Wahba problem) is formulated as follows: let us define an orthogonal matrix **A** with a determinant equal to +1, which minimizes the quadratic index

$$L(\mathbf{A}) = \tfrac{1}{2}\Sigma a_i |\mathbf{b}_i - \mathbf{A}\mathbf{r}_i|^2,$$

where the non-negative numbers a_i are the weighing coefficients. It has been strictly proved that the solution of this problem is the optimal quaternion $\boldsymbol{\Lambda} = (\lambda_0, \boldsymbol{\lambda})$, $\boldsymbol{\lambda} = \{\lambda_i, i = 1 \div 3\}$ that is equivalent to the required orthogonal matrix **A** and is defined as an eigenvector of the matrix **K** with the maximum eigenvalue $q_{\max}$, e. g. by relations

$$\mathbf{z} = \Sigma\, a_i \mathbf{b}_i \times \mathbf{r}_i; \quad \mathbf{B} = \Sigma\, a_i \mathbf{b}_i \mathbf{r}_i^{\mathrm{t}}; \quad \mathbf{S} = \mathbf{B} + \mathbf{B}^{\mathrm{t}};$$
$$\mathbf{K} = \begin{bmatrix} \mathrm{tr}\,\mathbf{B} & \mathbf{z}^{\mathrm{t}} \\ \mathbf{z} & \mathbf{S} - \mathbf{I}_3 \mathrm{tr}\mathbf{B} \end{bmatrix}; \quad \mathbf{K}\,\boldsymbol{\Lambda} = q_{\max}\,\boldsymbol{\Lambda}. \tag{29}$$

Relations (29) represent the QUEST algorithm for a quaternion's estimation, that is further applied for processing the measuring information obtained in the ACAC mode. The quaternion $\boldsymbol{\Lambda} = (\lambda_0, \boldsymbol{\lambda})$ is an one-one related

to the Rodrigues modified parameters' vector $\boldsymbol{\sigma}$ by the explicit analytic relations

$$\boldsymbol{\sigma} = \frac{\boldsymbol{\lambda}}{1+\lambda_0};\ \lambda_0 = \frac{1-\sigma^2}{1+\sigma^2};\ \boldsymbol{\lambda} = \frac{2\boldsymbol{\sigma}}{1+\sigma^2}\,. \qquad (30)$$

These relations permit transforming a problem on smoothing the quaternion data to standard task on smoothing the vector measurements.

5.3 A Vector Extrapolation

To the well-known direct and backward quaternion kinematic equations there correspond the direct and backward kinematic equations for the Rodrigues vector

$$\dot{\boldsymbol{\sigma}} = \frac{1}{4}\{\mathbf{I}_3(1-\sigma^2) + 2[\boldsymbol{\sigma}\times] + 2\boldsymbol{\sigma}\boldsymbol{\sigma}^{\mathrm{t}}\}\boldsymbol{\omega};$$
$$\boldsymbol{\omega} = 4\{\mathbf{I}_3(1-\sigma^2) - 2[\boldsymbol{\sigma}\times] + 2\boldsymbol{\sigma}\boldsymbol{\sigma}^{\mathrm{t}}\}\dot{\boldsymbol{\sigma}}/(1+\sigma^2)^2\,. \qquad (31)$$

A problem on extrapolation of the SC angular rate vector at the time interval T_n by the values of a vector $\boldsymbol{\omega}_s \equiv \boldsymbol{\omega}(t_s)$ given at discrete time moments $t_s \in \mathrm{T}_n$ with a period $T_q = t_{s+1} - t_s$, where $s = 0, 1, 2...n_q \equiv 0 \div n_q$ and $n_q = T_n/T_q$, consists in calculation of a time vector function $\mathbf{p}(t)$, which defines approximately the angular rate vector $\boldsymbol{\omega}(t)\ \forall\ t \in \mathrm{T}_n$ at the condition $\mathbf{p}_s = \boldsymbol{\omega}_s$.

In the general case, the extrapolation of values $\boldsymbol{\omega}_k$ at the time moments $t_k \in \mathrm{T}_n$ with a step $T_a = t_{k+1} - t_k$ and the multiplicity of periods $k_q^a \equiv T_a/T_q \geq 1$ can be applied.

Extrapolation of the quaternion values $\boldsymbol{\Lambda}_k$ given discretely by the quaternion $\mathbf{M}(t)\ \forall t \in \mathrm{T}_n$ is carried out as follows. At first, on the basis of biunique connection of the quaternion $\boldsymbol{\Lambda}$ with the Rodrigues vector $\boldsymbol{\sigma}$, using explicit analytic relations (30), the sequence of values for the vector $\boldsymbol{\sigma}_k$ is calculated. Then the extrapolation procedure presented above is applied to this sequence. At last, the inverse transformation to the quaternion $\mathbf{M}(t)$ is carried out using explicit relations (30).

The numerical calculations were carried out with applying filtration of the telescope attitude quaternion estimations (precisely, estimations of the Rodrigues vector) by the Savitsky – Goley method. The obtained results indicated that such a measuring basis is quite sufficient for restoring the base $\mathbf{S}$ actual position with respect to the base $\mathbf{I}$ at the QMD on determination of a turn angle $\delta\phi_{\mathrm{x}}$ about the OT optical axis no more than $1''$.

5.4 Calibration of a SINS

The problems of a strapped-down inertial navigation system (SINS) algorithmic software are connected with integration of kinematic equations in using the information on the quasi-coordinate increment vector $\mathbf{i}^{\omega}$obtained by the inertial block (IB) over the main discrete period T_u, filtering noises, identification and compensation of errors on a mutual angular position of the IB and the astronomical system (AS) reference frames, variation of the measure scale coefficients, and the IB bias with respect to the angular rate.

As kinematic parameters use is made of the quaternion $\Lambda = (\lambda_0, \lambda)$, the vector of Euler's parameters $\mathbf{L} = \{l_0, \mathbf{l}\}$, the orientation matrix $\mathbf{C}$, the Euler vector $\phi = \mathbf{e}\ \theta$, the

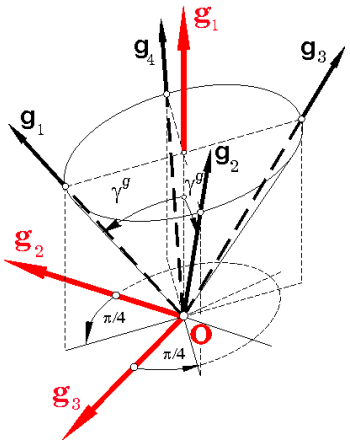

Fig. 11. The base $\mathbf{G}$

vector of terminal rotation $\theta = 2\mathbf{e}\ \mathrm{tg}(\theta\ /\ 2)$. For little variation of the angle θ and fixed direction of the Euler axis unit $\mathbf{e}$, the integration of the kinematic relations for the Euler vector $\phi(t)$ with obtaining the values $\Lambda_k \equiv \Lambda(t_k)$ was carried out by the following scheme:

$$\boldsymbol{\phi}_{k+1} = \theta_{k+1}\mathbf{e}_{k+1} \equiv \mathbf{i}_{k+1}^{\omega} = \int_{t_k}^{t_{k+1}} \boldsymbol{\omega}(\tau)d\tau \equiv \mathbf{Int}(t_k, T_u, \boldsymbol{\omega}(t));$$

$$t_{k+1} = t_k + T_u, \boldsymbol{\phi}_k \equiv \boldsymbol{\phi}(t_k) \Rightarrow \mathbf{C}_k \Rightarrow \boldsymbol{\Lambda}_k, \quad k \in \mathbb{N}_0.$$

Here the problems on the identification of the IB and the AS reference frames' "alignments" (errors on their mutual angular position) and variation of the measure scale coefficients by the vector $\omega(t)$ into the IB reference frame at forming the vectors $\mathbf{i}_{k+1}^{\omega}$ are the most complicated ones. This is due to a multiplicative character of the interconnected parametric disturbances indicated.

We introduce the IB virtual base $\mathbf{G} = \{\mathbf{g}_1, \mathbf{g}_2, \mathbf{g}_3\}$, which is computed by processing the measuring information from the integrating gyro sensors (for example, fiber-optic gyros), see Fig. 11. Let in a real time scale the measured values of vector $\mathbf{i}_{m\ l+1}^{g\ \omega}$, $l \in \mathbb{N}_0$ be obtained from the IB with the period $T_l << T_u$, and from the AS — the measured values of quaternion $\boldsymbol{\Lambda}_n^a$, $n \in \mathbb{N}_0$ with the period $T_o >> T_u$, moreover, the discrete periods T_o, T_u and T_l are multiple ones. Here the IB and the AS mathematical models have the form

$$\mathbf{i}_{m\ l+1}^{g\ \omega} = \mathbf{Int}(t_l, T_q, \boldsymbol{\omega}_m^g(t)) + \boldsymbol{\delta}_{l+1}^n;$$
$$\boldsymbol{\omega}_m^g(t) = (1-m)(\mathbf{I}_3 - [\Delta\times])(\boldsymbol{\omega}(t) - \mathbf{b}^g); \qquad (32)$$
$$\boldsymbol{\Lambda}_{m\ n}^a = \boldsymbol{\Lambda}_n \circ \boldsymbol{\Lambda}_n^n;$$

where vector $\boldsymbol{\omega}_m^g(t)$ presents the factual measured vector of angular rate into the base $\mathbf{G}$ with regard to unknown small and slow variations of the IB bias vector $\mathbf{b}^g$, the vector $\boldsymbol{\Delta} = \{\Delta_x, \Delta_y, \Delta_z\}$ of the "distort" angles and the IB scale coefficient m. In relations (32) the discrete noises $\boldsymbol{\delta}_{l+1}^n$ and $\boldsymbol{\Lambda}_n^n$ are taken into account for the IB and the AS output signals, accordingly.

The problem consists in developing the algorithms for estimation of values Λ_k, $k \in \mathbb{N}_0$ and simultaneous calibration of the SINS with filtering the noise vector $\boldsymbol{\delta}_{l+1}^n$, identification and compensation of the vectors $\boldsymbol{\Delta}$, $\mathbf{b}^g$ and the scale coefficient m variation.